

BLOOD FLOW IN SIMPLE MICROCHANNELS

Wesley Chang (1,3), David Trebotich (1,3), Luke P. Lee (2,3), Dorian Liepmann (2,3)

(1) Department of Mechanical Engineering, University of California, Berkeley 94720-1740 USA, tel: (510) 643-1099, email: wchang@bsac.eecs.berkeley.edu

(2) Department of Bioengineering Engineering, University of California, Berkeley 94720-1774

(3) Berkeley Sensor and Actuator Center, 497 Cory Hall, Berkeley, CA 94720-1774

Abstract – Development of medical micro-assay systems must be based on an understanding of blood flow mechanics at scales of tens to hundreds of microns. This study investigated the use of a simple power law model for blood flow of between 2.5 and 100 $\mu\text{l}/\text{min}$ in channels with 200 x 60 μm cross-sections and the following configurations: straight, 90 degree bend, and sudden contraction from 200 to 100 μm . Experimental measurements of pressure vs. flow rate for blood flow in these channels were compared to predictions generated by CFD simulations. The experiments and simulations were consistent in their predictions of the magnitude of hydrodynamic resistances of the channels and the slight non-linearity of pressure vs. flow in each of the channel configurations.

I. INTRODUCTION

Medical micro-assay systems (lab-on-a-chip) are being developed to perform rapid clinical chemistry using minimal sample sizes. Such systems will vastly improve medical diagnosis and patient monitoring by eliminating the often slow and cumbersome processes of conventional clinical laboratories. The basic operations of these miniature assay devices will involve the transport and manipulation of blood and blood components at dimensions of tens to hundreds of microns and in volumetric rates of around 1-10 $\mu\text{l}/\text{sec}$ [1]. Development of various microfluidic components to process blood in these devices must be based on a firm understanding of its non-Newtonian properties at these dimensions. This understanding will permit determination of fluid flow resistances within fluidic components as well as quantification of the high fluid shear forces incurred on blood constituents in flows through irregular geometries. It has long been established that blood is “shear thinning”: viscosity decreases as shear rate increases. But while many constitutive equations have been demonstrated for blood [2-4], the validity of existing models for different flow geometries at the microscale—where the continuum assumption becomes tenuous—remains untried.

Existing models for blood can be categorized as either some variation of the power law equation or as some Casson-like equation [4]. Both types model the dependence of blood viscosity with respect to shear rate, and Casson-like models even account for non-zero yield stresses,

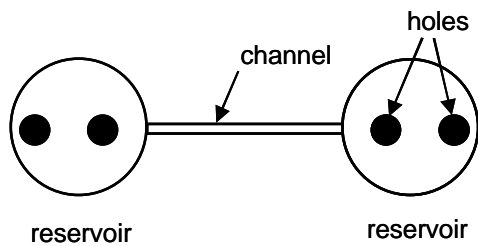
stresses that must be exerted before blood will shear. However, yield stresses for blood are observed only with static or low shear experiments. Based on the expected flow rates and dimensions of microfluidic components [3], the shear stresses generated in these devices will be very high, far exceeding the hypothesized yield stresses for blood. When yield stress is negligible, most Casson-like models simplify to some form of the power law. This study will therefore evaluate the use of the power law model to representing blood flow in prospective micro-flow geometries by comparing measured fluid mechanical resistances in these flow geometries with the flow parameters predicted from numerical simulations of the power law constitutive equation. The specific objectives of this study are: 1) to measure pressure drop versus volumetric flow rate for blood flow through channels with the following traces: 200 μm x 60 μm straight, 200 μm x 60 μm to 100 μm x 60 μm sudden contraction, and 200 μm x 60 μm sudden, 90° bend; and 2) to numerically compute pressure vs. flow rate relations for these flow configurations based on simulations of flow of a power law model for blood.

II. METHODS

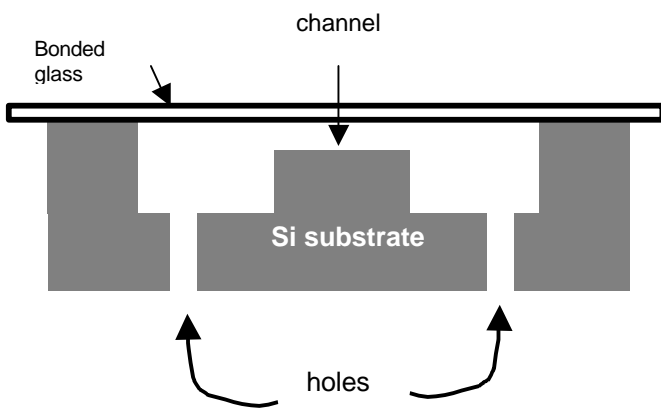
The channels for flow testing were fabricated in silicon using deep reactive ion etching (DRIE) to create rectangular cross-section trenches. (Fig. 1) Straight channels, channels with sudden contractions, and channels with 90° bends were all were etched 60 μm deep into the silicon and had total lengths of 12mm, regardless of configuration. Both the straight channel and 90° bend were patterned with 200 μm widths, while in the channel with sudden contraction, a 200 μm wide, 6mm long channel fed into a 100 μm wide, 6mm long channel. Fluid reservoirs along with 1mm diameter through-substrate interconnect holes were also etched into the silicon substrate at both ends of each channel to facilitate the insertion and removal of fluid. The trenches and reservoirs were sealed by anodically bonding Pyrex glass over the top of the substrate. Each flow device was clamped into an interconnecting fixture, which allowed fluid to be

delivered from external tubing into the through-holes of the flow device without any leakage of fluid.

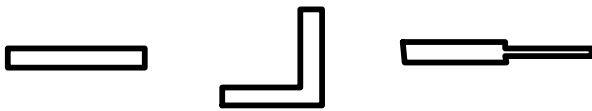
(a) Top view of flow device



(b) Side cross-sectional view



(c) Top view of channels: straight, bend, and contraction



(d) Electron micrographs

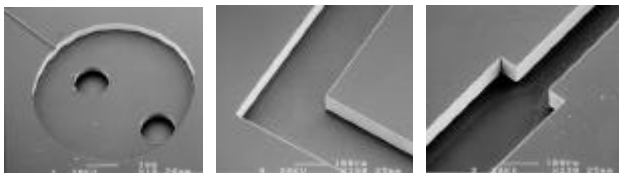


Fig. 1 Flow structures. (a,b) The entire flow structure consisted of the channel which connects to circular reservoirs at both ends. Interconnect holes are etched through the substrates to allow fluid to enter or drain from the reservoirs. A glass slide is anodically bonded over the channels and reservoirs to seal the structure. (c) Channel configurations include straight channels, 90° bends, and sudden contractions. (d) Micrographs of reservoir, bend, and contractions etched into silicon and prior to bonding of glass coverslip.

Defibrinated sheep blood of 41% hematocrit (cell volume fraction) was obtained from a local scientific vendor (Hemostat Laboratories). The blood was refrigerated at around 5°C immediately following harvest and was shipped and stored at that temperature. The blood was used for experiments within two weeks of harvest and warmed to 23°C for both viscometry and flow testing.

To perform the flow testing, the blood was pumped through the flow structures via the interconnecting fixture at explicit volumetric flow rates ranging from 2.5 to 100 $\mu\text{l}/\text{min}$ by a syringe pump (Cole-Parmer). After passing through the device, the fluid drains to atmospheric pressure. The pressure head generated across the flow structure by the explicit flow rate was measured off-chip and upstream of the device by a Honeywell Microswitch flow-through pressure transducer (Honeywell Corp.). It was determined that the combined fluid resistances of the interconnecting fixture and the substrate reservoir was negligible—on the order of 0.1% of the resistances of the test channels.

From the earlier discussion, the constitutive equation chosen for this study was the power law equation, which has the form:

$$\tau = k(\dot{\gamma})^n$$

The specific parameters for blood used in this study were determined from a least squares fit of the log-log relation between shear rate and shear stress, which was complied from direct viscometry of the blood. The viscometry was performed by a Vilastic 3 Viscoelastic Analyzer (Vilastic Scientific, Inc.), which measures fluid parameters of a sample as it is oscillated in a small tube [5].

Steady state flows of both the power law models a Newtonian reference were numerically simulated for each of the flow geometries by CFD-ACE+ software, a pressure-based, finite volume flow solver (CFD Research Corporation). Using the chosen power law flow, the simulation was performed with explicit volumetric flow rates, and resulting pressure generated between inlet and outlet of the flow structure was computed.

To provide a comparison between an established constitutive model and the model formulated specifically for this study, simulations of blood flow through the straight channel and channel with 90° bend were also performed using the “one variable” power law of Walburn and Schneck [3], which had the parameters $n=0.785$ and $k=0.0134 \text{ Pa}\cdot\text{s}^n$, obtained at 37°C. The Walburn-Schneck model has a greater degree of non-Newtonian character than the power law model developed in this study.

III. RESULTS

A. Viscometry

Defibrinated sheep blood is a shear thinning fluid, with the viscosity dropping from 5.4×10^{-3} to just under $4.9 \times 10^{-3} \text{ Pa}\cdot\text{s}$ over the shear rate range of 80 to 400s^{-1} (Fig. 2). These values are comparable to the measurements of blood viscosity in the literature [2]. Least-squares linear fit of the shear stress vs. shear rate yielded the values for the power law parameters: $k = 0.00733 \text{ Pa}\cdot\text{s}^n$, and $n = 0.932$. These values were used in the CFD simulations. Based on these parameters, this blood is only weakly non-Newtonian, especially at high shear rates.

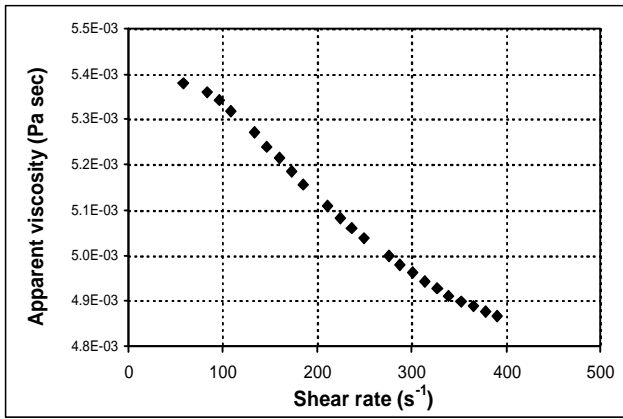


Fig. 2. Dependence of blood viscosity on shear rate. Direct measurement of blood viscosity was performed on a oscillating tube microrheometer. The measurements of blood viscosity corresponds to power law parameters of $k=0.00733 \text{ Pa}\cdot\text{s}^n$ and $n=0.932$.

B. Flows Experiments

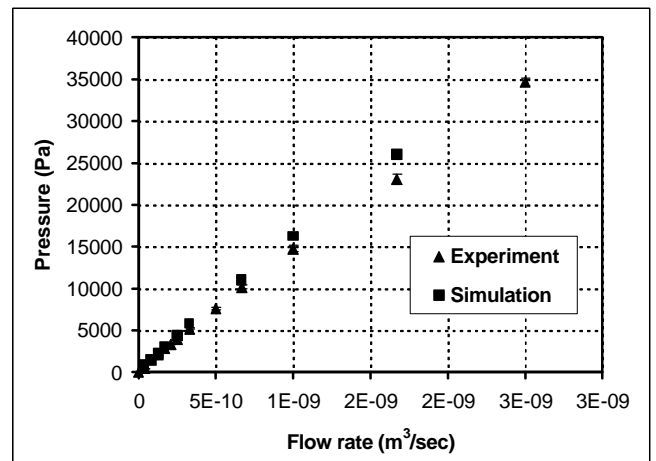
The pressure vs. flow rate relationships for all of the channel configurations were roughly linear, though the flow resistances were somewhat higher for lower flow rates than for higher flow rates, as would be expected for a shear thinning fluid. For the $200\mu\text{m} \times 60\mu\text{m} \times 12 \text{ mm}$ straight channel, the first-order estimation of flow resistance for blood was about $1.3 \times 10^{13} \text{ kg}/(\text{s}\cdot\text{m}^4)$ roughly 3.5 times that for water. The addition of the ninety degree bend midway through the channel increases the flow resistance to about $1.8 \times 10^{13} \text{ kg}/(\text{s}\cdot\text{m}^4)$, while with a sudden contraction midway and subsequent width reduction to $100\mu\text{m}$, the flow resistance was about $2.5 \times 10^{13} \text{ kg}/(\text{s}\cdot\text{m}^4)$.

C. Simulations

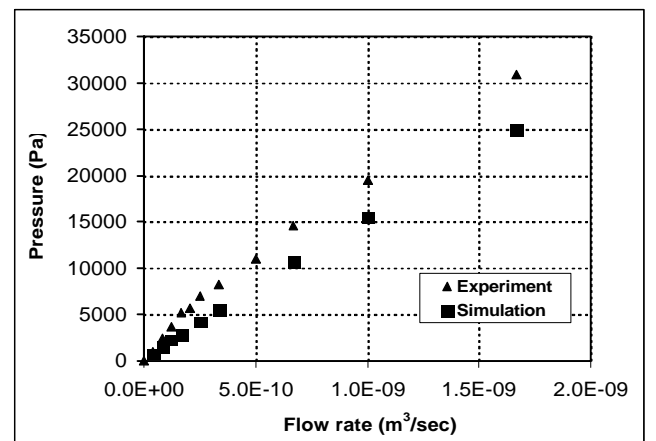
Simulations of the flow through the channels using the chosen power law model produced pressure vs. flow rate relationships that were similar to the trends and magnitude of experimentally determined relationships. As with the experimental measurements, the computed relationships between pressures vs. flow rates were roughly linear. With both the straight channel and the channel with sudden contraction, results of numerical simulations closely matched the experimental measurements (Fig. 3a,c). Simulations of the flow through the channel with the bend, however, predicted pressure drops that were consistently smaller than the pressure drops measured during flow experiments (Fig. 3b).

Not surprisingly, simulations using the Walburn-Schneck model for blood flow through the straight channel and channel with bend produced pressure vs. flow relationships that deviated more from linear than relationships produced with our power law model. Hydrodynamic resistances (slopes in Fig. 4) were visibly lower for higher flow rates than they were for lower flow rates. Overall, the flow resistance were much lower for the Walburn-Schneck model than for our model, since the high shear viscosity predicted the former are much lower.

(a) Straight channel: $200\mu\text{m} \times 60\mu\text{m} \times 12\text{mm}$



(b) Bend: $200\mu\text{m} \times 60\mu\text{m} \times 6\text{mm} \rightarrow 90^\circ \text{ bend} \rightarrow 200\mu\text{m} \times 60\mu\text{m} \times 6\text{mm}$



(c) Sudden contraction: $200\mu\text{m} \times 60\mu\text{m} \times 6\text{mm} \rightarrow 100\mu\text{m} \times 60\mu\text{m} \times 6\text{mm}$

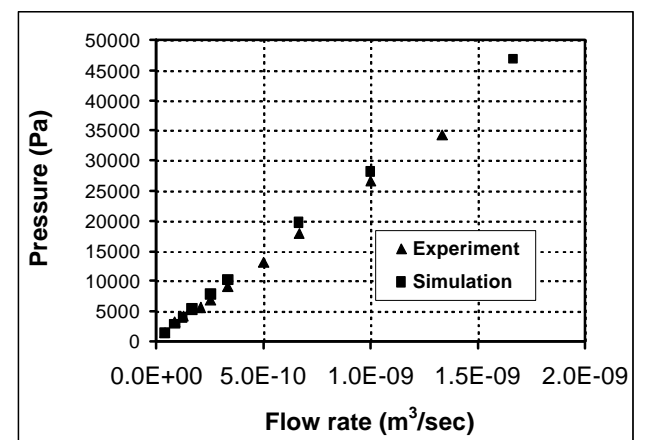
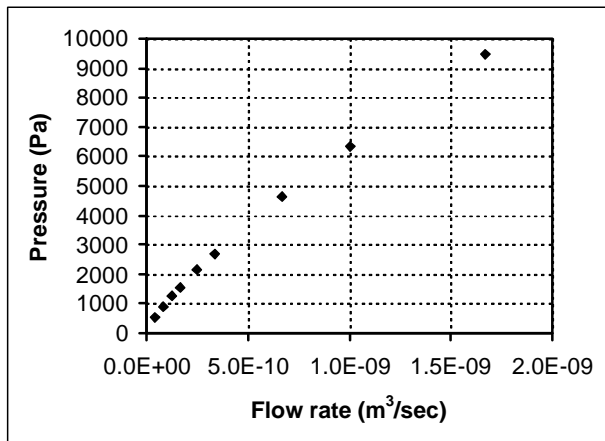


Fig. 3. Pressure vs. flow rate relationships. Both experimental measurements and simulation results with our power law model are shown.

(a) Straight channel: $200\mu\text{m} \times 60\mu\text{m} \times 12\text{mm}$



(b) Bend: $200\mu\text{m} \times 60\mu\text{m} \times 6\text{mm} \rightarrow 90^\circ \text{ bend} \rightarrow 200\mu\text{m} \times 60\mu\text{m} \times 6\text{mm}$

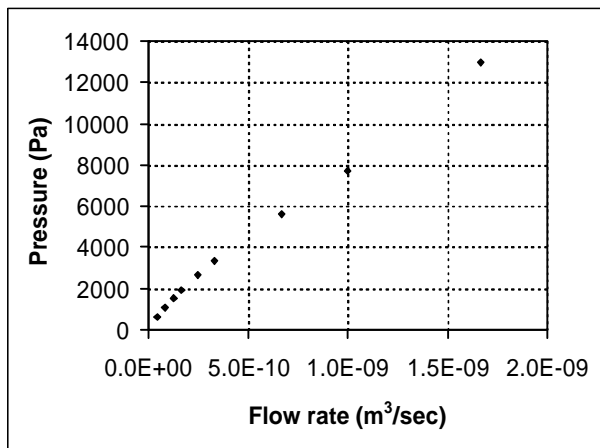


Fig. 4. Simulations of pressure vs. flow rate relationships using the one variable Walburn-Schneck power law.

IV. DISCUSSION

While blood has been extensively studied, most of the investigations have dealt with either macroscopic flows through arteries and veins or microscopic flows in capillaries, where the motion of individual cells is accounted for explicitly. The so-called “mesoscopic” regime, at the scale of tens to hundreds of microns is the most difficult to study. While the population of cells is too great to account for them individually, the continuum assumption may not apply in many cases, as the cell dimensions are a significant fraction of the characteristic flow dimensions. Efforts to develop and verify modeling techniques for mesoscopic flow will be aided by the use of microfabrication technology to create specific flow geometries with sizes ranging from the mesoscopic regime to the scale of individual cells.

This study investigated blood flow through three simple

“mesoscopic” geometries at flow rates expected for micro-analysis systems. Our results indicate that at the high shear rates expected for microfluidic devices, the flow resistances of blood in simple fluidic geometries does decrease somewhat as flow rates are increased. But the relationships between pressure head and flow rate are at worst only weakly non-linear. This result is consistent with predictions of fluid resistances by numerical modeling using a simple power law equation, validating the use of this model for simple geometries at scales of around 100-200 μm . Additionally, simulations with the well-established Walburn-Schneck power law model, which is strongly non-Newtonian, also seemed to indicate that despite the weak non-linearity of pressure vs. flow rate, a linear fit can provide a reasonable first-order estimation of the relationship between flow rates and driving pressure. This study therefore suggests that modeling of blood in these flow configurations and with dimensions of hundreds of microns can in some cases be performed with simple constitutive models, although further refinement in the simulation method is needed before this can be confirmed.

Studies on shear-induced hemolysis have indicated that direct fluid mechanical shearing beyond a threshold of 150–450 Pa, depending on duration of exposure to shear, can incur extensive cell damage [6]. Given the viscosity of blood, this shear stress corresponds to a shear rate of around 30,000–90,000 s^{-1} . The flows produced in these experiments produced shear rates on the order of 10,000-50,000 s^{-1} , raising the possibility that some damage may have been incurred upon blood cells, even in these simple geometries.

While in actual assay devices, whole blood will be collected and manipulated, the blood used in this study was defibrinated, lacking fibrin, a protein essential for the aggregation of blood cells. The presence of this protein, through its role in aggregating cells is in part responsible for the higher apparent viscosity of blood at low shear rates [2, 7]. When cell aggregation is eliminated, the viscosity of the blood changes less as shear rate is varied, since it has lower viscosity than whole blood at low shear rates but similar viscosity at high shear rates [7]. Because of the expected similarity in viscosity of whole blood and defibrinated blood at high shear rates, the difference between our power law model and the “one variable” model of Walburn and Schneck can probably be attributed mostly to the difference in temperatures at which the blood was evaluated, 23 $^\circ\text{C}$ for the former and 37 $^\circ\text{C}$ for the latter. Given the high shear rates of microfluidic devices, it is probably reasonable to use defibrinated blood to represent the behavior of whole blood, particularly at the higher flow rates, although the present study did not directly prove this.

Another shortcoming in this study was that the Fahraeus effect was not account for. When a large reservoir of blood feeds into tubes smaller than about 200 μm , there is a tendency for hematocrit within the tubes to decrease, this effect becoming progressively more pronounced with smaller tubes [8]. With lower hematocrit within the tubes, blood appears less viscous—the Fahraeus-Lindquist effect. While the Fahraeus effect for

blood flow into rectangular channels has not been quantified (as opposed to tubes with circular cross-sections), the scales used in this study, cross-sectional area of our 200 μm x 60 μm channel are likely to at least be at the upper fringe of the regime in which the Fahraeus effect takes effect, and the hematocrit of blood within channels may be somewhat lower than the 41% value in the feed reservoirs. This decrease was not explicitly addressed in formulating our model for blood and may not be an important effect for the particular flow conditions in this study. But future studies should address this phenomenon, especially when smaller flow scales are investigated.

Limitations in the fineness of grid sizes in the numerical models of the flow invariably result in residual errors in computing pressure vs. flow rates. Such errors may invariably be in part responsible for the discrepancy between experimental measurements and predictions, especially in the channel with the sudden bend. The sudden bend is a geometry that tests the limits of numerical integration methods.

While this study is among the first to explicitly measure flow parameters of blood in microfabricated devices, it is merely a prelude to more rigorous studies, which will examine the microstructure of flows through a greater variety of geometries and scales. This study considered only the whole hydrodynamic *resistances* of three simple channel geometries. Future studies will map velocity and shear rate profiles within the flow geometries. More advanced work will even account for expected changes in local hematocrit in various flow geometries. Additionally, it will be important to observe the orientation, deformation and hemolysis of blood cells subject to different flow conditions involving high shear

rates. The knowledge obtained from these studies will set important guidelines for designing and configuring various microfluidic devices to support development of lab-on-a-chip assay systems.

ACKNOWLEDGMENT

This study was supported by the Defense Advanced Research Projects Agency's (DARPA) μ FLUMES program. It was also funded by a Whitaker Foundation Graduate Fellowship. All devices were fabricated in the UC Berkeley Microfabrication Facility.

REFERENCES

- [1] Petersen, K.E., *et al.*, "Toward next generation clinical diagnostic instruments: scaling and new processing paradigms" *J Biomed Microdev*, 1998. **1**(1): p. 71-79.
- [2] Fung, Y.C., *Biomechanics: Mechanical properties of living tissue*. 2nd ed. 1993, New York: Springer-Verlag.
- [3] Walburn, F.J. and D.J. Schneck, "A constitutive equation for whole human blood" *Biorheology*, 1976. **13**: p. 201-210.
- [4] Zhang, J.-B. and Z.-B. Kurang, "Study on blood constitutive parameters in different blood constitutive equations" *J Biomech*, 2000. **33**: p. 355-360.
- [5] Thurston, G., "Theory of oscillation of a viscoelastic fluid in a circular tube". *J Acoustical Soc Amer*, 1960. **32**(2): p. 210.
- [6] Leverett, L.B., *et al.*, "Red blood cell damage by shear stress" *Biophys J*, 1972. **12**: p. 257-273.
- [7] Chien, S., "Shear dependence of effective cell volume as a determinant of blood viscosity" *Science*, 1970. **168**: p. 977-979.
- [8] Barbee, J.H. and G.R. Cokelet, "The Fahraeus effect". *Microvasc Res*, 1971. **3**: p. 6-16.